J|A|C|S
ARTICLES
Published on Web 03/18/2003

Intermodular Communication in Modular Polyketide Synthases: Structural and Mutational Analysis of Linker Mediated Protein−Protein Recognition

Pawan Kumar,[†] Qing Li,[‡] David E. Cane,[§] and Chaitan Khosla*,[†,‡,||]

Contribution from the Departments of Chemical Engineering, Chemistry, and Biochemistry, Stanford University, Stanford, California 94305 and Department of Chemistry, Brown University, Providence, Rhode Island 02912

Received December 16, 2002; E-mail: ck@chemeng.stanford.edu

Abstract: Modular polyketide synthases (PKSs) present an attractive scaffold for the engineered biosynthesis of novel polyketide products via recombination of naturally occurring enzyme modules with desired catalytic properties. Recent studies have highlighted the pivotal role of short intermodular "linker pairs" in the selective channeling of biosynthetic intermediates between adjacent PKS modules. Using a combination of computer modeling, NMR spectroscopy, cross-linking, and site-directed mutagenesis, we have investigated the mechanism by which a linker pair from the 6-deoxyerythronolide B synthase promotes chain transfer. Our studies support a "coiled-coil" model in which the individual peptides comprising this linker pair adopt helical conformations that associate through a combination of hydrophobic and electrostatic interactions in an antiparallel fashion. Given the important contribution of such linker pair interactions to the kinetics of chain transfer between PKS modules, the ability to rationally modulate linker pair affinity by site-directed mutagenesis could be useful in the construction of optimized hybrid PKSs.

Modular polyketide synthases (PKSs) are multifunctional enzyme systems in which domains responsible for catalysis of individual steps in the biosynthesis of polyketide products are organized in a modular fashion. For example, 6-deoxyerythronolide B synthase (DEBS) catalyzes the biosynthesis of 6-deoxyerythronolide B (**1**), the aglycon precursor of the antibiotic erythromycin. DEBS comprises three large proteins (>300 kDa each), designated DEBS1, DEBS2, and DEBS3. Each protein consists of two modules as shown in Figure 1A. Each module contains at least three essential domains, namely, acyl transferase (AT), acyl carrier protein (ACP), and keto synthase (KS) domains. The AT catalyzes transfer of extender units from methylmalonyl-CoA precursors to the ACP, whereas the KS domain is responsible for catalyzing decarboxylative condensation of the extender unit to the growing polyketide chain.[1,2] Additional domains such as ketoreductases (KR), dehydratases (DH), and enoyl reductases (ER) are responsible for postextensional modifications of the polyketide chain.

Naturally occurring PKS modules exhibit an impressive spectrum of catalytic variety and stereoselectivity. The ability to predictably harness this diversity for the construction of complex natural product-like molecules is a major goal of our research. As a prerequisite it is important to understand the mechanistic basis for selective chain transfer between adjacent modules in a multimodular PKS. Previous studies[3−6] have revealed that small, nonconserved segments of amino acid residues at the N- and C-termini of the three DEBS polypeptides play an important role in protein−protein recognition and hence in the specificity of interpolypeptide chain transfer (Figure 1A). To understand the mechanism of protein−protein recognition, these linker regions were subjected to structural and mutational analysis. Our experiments provide compelling evidence for an antiparallel "coiled-coil" mode of interaction and pinpoint the precise regions of the linkers that interact to promote intermodular chain transfer.

Results

Proposed Model for Linker Interactions. As summarized in the Materials and Methods section, a coiled-coil model for interactions between M2C (the linker peptide at the C-terminus of module 2) and M3N (the linker peptide at the N-terminus of module 3) was constructed and is shown in Figure 2A. This model was originally developed based on the recognition of a heptad repeat of hydrophobic residues in the primary sequences of both linker regions by the PAIRCOIL program.[4,7] As predicted for coiled coils, these linker pairs also have hydrophilic

[†] Department of Chemical Engineering, Stanford University.
[‡] Department of Chemistry, Stanford University.
[§] Brown University.
[||] Department of Biochemistry, Stanford University.

(1) Cortes, J.; Haydock, S. F.; Roberts, G. A.; Bevitt, D. J.; Leadlay, P. F. *Nature* **1990**, *348*, 176−178.
(2) Donadio, S.; Staver, M. J.; McAlpine, J. B.; Swanson, S. J.; Katz, L. *Science* **1991**, *252*, 675−679.
(3) Gokhale, R. S.; Tsuji, S. Y.; Cane, D. E.; Khosla, C. *Science* **1999**, *284*, 482−485.
(4) Tsuji, S. Y.; Cane, D. E.; Khosla, C. *Biochemistry* **2001**, *40*, 2326−2331.
(5) Wu, N.; Tsuji, S. Y.; Cane, D. E.; Khosla, C. *J. Am. Chem. Soc.* **2001**, *123*, 6465−6474.
(6) Wu, N.; Cane, D. E.; Khosla, C. *Biochemistry* **2002**, *41*, 5056−5066.
(7) Berger, B.; Wilson, D. B.; Wolf, E.; Tonchev, T.; Milla, M.; Kim, P. S. *Proc. Natl. Acad. Sci. U.S.A.* **1995**, *92*, 8259−8263.

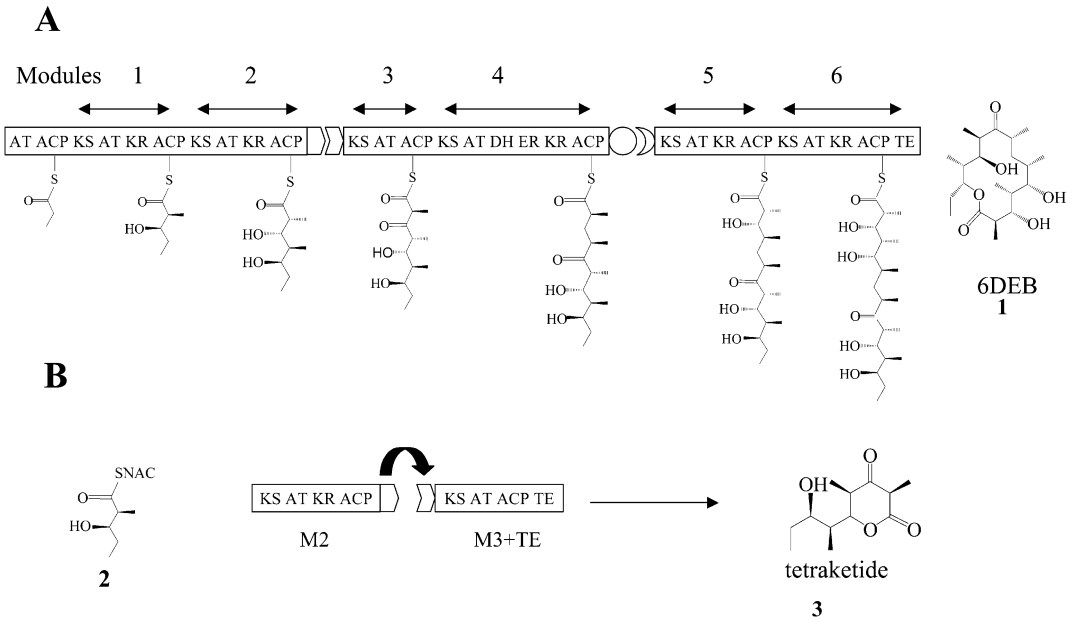

Figure 1. (A) Schematic diagram of the biosynthesis of 6-dEB (**1**) by 6-deoxyerythronolide B synthase. Each polypeptide, DEBS1, DEBS2, and DEBS3, contains two modules, and each module comprises a set of active-site domains responsible for addition and modification of an extender unit. The short linker regions are located at the N- and C-termini; their shapes exemplify the complementarity demonstrated by each pair. (B) Reconstitution of chain transfer between modules 2 and 3 of DEBS. Compound **2** primes M2 and undergoes one round of extension. The resulting triketide is transferred to M3+TE. In this module another chain extension takes place, and the resulting tetraketide (**3**) is released and cyclized by the terminal TE domain.

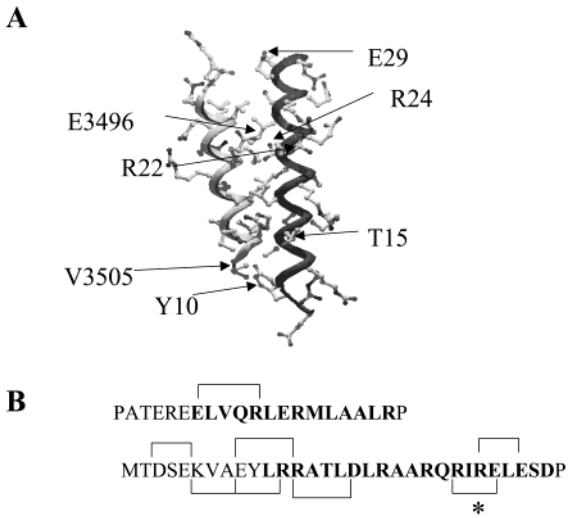

Figure 2. (A) Computer-generated coiled-coil model for the M2C−M3N interaction. Key residues discussed in the text are shown. (B) Potential *intra*helical ion pairs in the two proposed coils. Both coils are capped with prolines, and regions on coils with heptad repeats are shown in boldface type. One i, $i + 3$ ion pair is broken as a result of the R24E mutation on the M3N linker, resulting in a less stable helix that may lead to reduced activity of this mutant M3+TE. This ion pair is shown by an asterisk.

surfaces that include suitably positioned complementary charged residues (Figure 2A). On the basis of literature precedents in the context of other coiled coils,[8−11] we therefore proposed that these coiled coils were stabilized by hydrophobic interactions, and that specificity derived from the ion-pair interactions between the two helices. It should, however, be noted that the predicted helix lengths in M2C and M3N are relatively short; this is consistent with experimental observations that DEBS1 and DEBS2 associate only weakly (estimated $K_D \sim 1\ \mu M$).[4] We therefore hypothesized that, to maximize interactions between M2C and M3N, the VL−LL hydrophobic face of M2C interdigitates into the LLI−AAL face of M3N (Figure 2A). In this proposed antiparallel orientation of the two helices, the charged residues are arranged such that residues in the M2C linker form ion pairs with oppositely charged residues in the M3N linker. Three kinds of experiments were performed to test this model. First, the helicity of a synthetic peptide based on the sequence of the M3N linker was evaluated by NMR spectroscopy. Second, mutants of ACP2 and M3+TE containing engineered cysteine residues were subjected to 1,3-dibromopropanone-mediated cross-linking. Finally, the ability of a polyketide chain to be transferred between selected pairs of wild-type and mutant forms of ACP2 and M3+TE was quantitatively analyzed. Our results from these experiments are described below.

NMR. The 2D NOESY spectrum of the M3N peptide is shown as Supporting Information. From the TOCSY spectrum of the peptide taken under identical conditions, we were able to assign most of the resolved peaks (see Supporting Information). NOE connectivities and deviation of H^{α} resonances from those of a random coil conformation are shown in Figure 3, panels A and B, respectively. Most of the residues display high-field shifted H^{α} chemical shifts, suggestive of helical structure in the peptide.[12] Strong $H^{N}_{(i)}$–$H^{N}_{(i+1)}$ peaks were observed between neighboring residues. In addition, short distances (<5 A) between protons $H^{\alpha}_{(i)}$ and $H^{N}_{(i+1,i+2,i+3,i+4)}$, $H^{N}_{(i)}$ and $H^{N}_{(i+2)}$, and $H^{\alpha}_{(i)}$ and $H^{\beta}_{(i+3)}$ were also deduced from observed NOEs. Together, these observations support our proposal that the M3N peptide has a propensity to a helical conformation.

Direct Evidence for Antiparallel Coiled-Coil Interactions from Cross-Linking Experiments. The cross-linking of neighboring pairs of thiol functional groups with suitable bifunctional

(8) O'Shea, E. K.; Rutkowski, R.; Kim, P. S. *Science* **1989**, *243*, 538−542.
(9) O'Shea, E. K.; Rutkowski, R.; Stafford, W. F.; Kim, P. S. *Science* **1989**, *245*, 646−648.
(10) O'Shea, E. K.; Rutkowski, R.; Kim, P. S. *Cell* **1992**, *68*, 699−708.
(11) Shu, W.; Liu, J.; Ji, H.; Lu, M. *J. Mol. Biol.* **2000**, *299*, 1101−1112.
(12) Wishart, D. S.; Sykes B. D.; Richards, F. M. *J. Mol. Biol.* **1991**, *222*, 311−333.

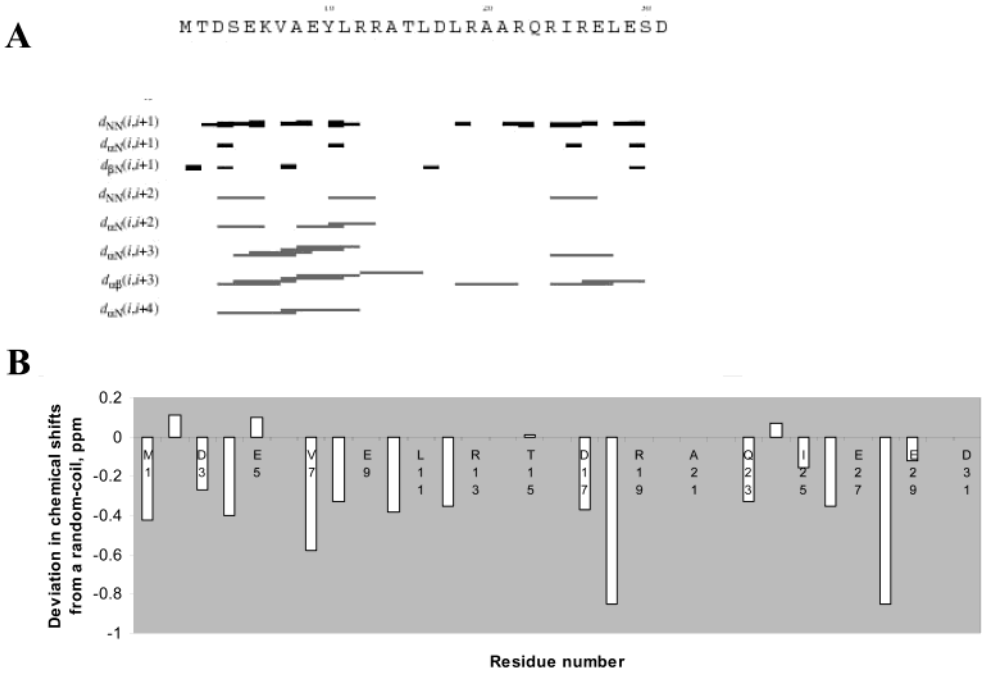

Figure 3. (A) Summary of ^{1}H NOE connectivities and peak intensities in terms of distance parameter *d*. The width of the bars represents the relative intensities (and hence relative distances) of the NOE cross-peaks connecting $H^N_{(i)}$ to $H^N_{(i+1,i+2)}$, $H^\alpha_{(i)}$ to $H^N_{(i+1,i+2,i+3,i+4)}$, $H^\beta_{(i)}$ to $H^N_{(i+1)}$, and $H^\alpha_{(i)}$ to $H^\beta_{(i+3)}$, which were determined in the 2D NOESY spectrum. (B) Deviation of H^α chemical shifts for various residues from random coil configurations. Upfield deviation of most amino acids is suggestive of helical conformation.

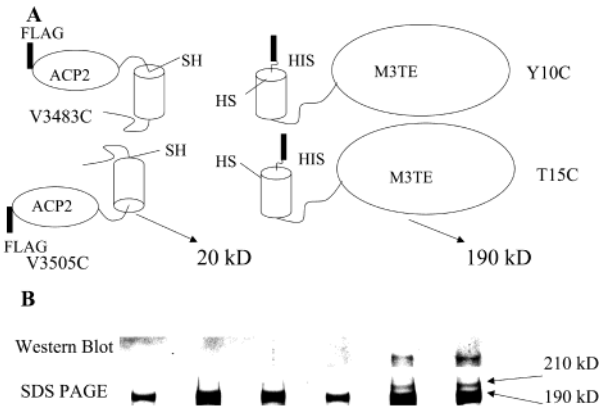

Figure 4. (A) Alternative models for the relative orientation of M2C and M3N. Cysteine residues were introduced such that specific cross-linking would be observed in certain cases but not in others. (B) Coomassie Blue stain and Western blot of equivalent cross-linking reactions. Lane 1, ACP2-(V3483C) and M3+TE (wt); lane 2, ACP2(V3483C) and M3+TE (Y10C); lane 3, ACP2(V3483C) and M3+TE(T15C); lane 4, ACP2(V3505C) and M3+TE (wt); lane 5, ACP2(V3505C) and M3+TE (Y10C); lane 6, ACP2-(V3505C) and M3+TE(T15C). Cross-linking was observed only in lanes 5 and 6, suggesting antiparallel orientation of coils. For ACP2, residue numbering is that for M2.

reagents is a common strategy for probing noncovalent protein−protein interactions. Toward this end, cysteine residues were engineered at selected positions in the linker regions of ACP2 and M3+TE proteins (Figure 4A). In particular, Y10 and T15, two residues located near the N-terminal end of the putative M3N helix, were alternately replaced with cysteines. Similarly, V3483C and V3505C mutants of ACP2 were constructed; V3483 is located near the N-terminus of the putative M2C helix, whereas V3505 is located near the C-terminal end of this helix. Depending upon the orientation and relative geometries of the two helices, it was anticipated that some ACP2−M3+TE pairs could be cross-linked by 1,3-dibromopropanone whereas other pairs would be unaffected by this bifunctional cross-linking reagent. Since M3+TE and ACP2 are 190 and 20 kDa proteins, respectively, a 210 kDa cross-linked product was expected between these two proteins. Such an adduct could be readily recognized by antibodies specific to distinct tags on ACP2 (FLAG-tagged) and M3+TE (hexa-His-tagged). Each mutant protein was expressed, purified, and assayed. No differences were observed between the catalytic properties of the wild-type and mutant proteins. However, as shown in Figure 4B, a dibromopropanone cross-linked product was observed only when ACP2(V3505C) was coincubated with M3+TE(Y10C) or M3+TE(T15C). No such adduct could be observed when ACP2(V3483C) was assayed in the presence of either of the M3TE mutants described above. Moreover, neither ACP2 mutant could be cross-linked to wild-type M3+TE under equivalent conditions. In addition to validating the proposed coiled-coil model for helix interactions between M2C and M3N, these results provide evidence the helices are oriented in an antiparallel fashion.

Effects of Altering Ionic Residues in the Linker Pairs on Intermodular Chain Transfer. Mutant forms of both M2 and M3+TE were engineered in which selected charged residues on the putative helices were replaced with residues of opposite charges. In particular, an E3496R mutant of M2 and an R24E mutant of M3+TE were constructed (Figure 2A), and tetraketide synthesis (Figure 1B) by different wild-type and mutant module pairs was monitored (Table 1). Consistent with an earlier report,[4] the observed velocity of tetraketide production for the wild-type M2 and M3+TE (1 μM each) was 0.15 min^{-1}. At similar protein concentrations, this rate decreased by more than 10-fold when the mutation R24E was introduced into the linker region of M3+TE. [Some, but not all, of this reduction could be due to the 2-fold reduced activity of the mutant M3+TE-(R24E) itself.] Loss of tetraketide productivity was partially

Table 1: Mutational Analysis of Intermodular Communication[a]

M2:M3TE (μM)	M2	M3+TE	V (μM product min^{-1}) 3	4	5
0:1	0	WT			0.33
0:1	0	R24E			0.16
0.5:0.5	WT	WT	0.04	0.01	0.04
0.5:0.5	E3496R	WT	0.07	0.03	0.01
1:1	WT	WT	0.15	0.03	0.07
1:1	E3496R	WT	0.15	0.06	0.01
1:1	WT	R24E	0.01	0.00	0.06
1:1	E3496R	R24E	0.03	0.00	0.05
3:1	WT	WT	0.11	0.03	0.02
3:1	E3496R	WT	0.14	0.07	0.09
3:1	WT	R24E	0.04	0.02	0.07
3:1	E3496R	R24E	0.07	0.03	0.03
1:3	WT	WT	0.30	0.06	0.22
1:3	E3496R	WT	0.31	0.10	0.04
1:3	WT	R24E	0.03	0.01	0.23
1:3	E3496R	R24E	0.09	0.02	0.16

[a] Rates of formation (V) of tetraketide (**3**), triketide (**4**), and triketide ketolactone (**5**) are listed.

compensated (3-fold) by introducing a compensating charge E3496R in the M2 linker. Curiously, the turnover number of M2(E3496R) and wild-type M3+TE was comparable to that of the wild-type module pair. In fact, at lower concentrations of each module (0.5 μM) the M2(E3496R) and wild-type M3+TE pair exhibited a higher velocity for tetraketide production than the wild-type pair, suggesting that the engineered module pair has a higher affinity than its wild-type counterpart.

Kinetic studies were also performed under conditions where one module was present in 3-fold excess over another. At 1:1 and 3:1 concentrations of wild-type M2:M3+TE the rates were similar, whereas at a 1:3 concentration ratio the velocity of tetraketide formation was enhanced. These results confirm earlier observations that at 1 μM the wild-type system is saturated with respect to M2 but not with respect to M3+TE.[4] Similar results were also observed for the M2(E3496R):M3+TE(wt) system. In contrast, for both the M2(wt):M3+TE(R24E) module pair and the M2(E3496R):M3+TE(R24E) module pair, a significant increase in reaction velocity was observed when either the M2-(wt or E3496R) concentration or the M3+TE(R24E) concentration was increased to 3 μM. Thus, it appears that the dissociation constant of the M2(E3496R):M3+TE(wt) pair is comparable to that of the wild-type module pair, whereas the dissociation constants of the M2(wt):M3+TE(R24E) and M2(E3496R):M3+TE(R24E) pairs have increased, indicating weaker binding.

Discussion

The importance of protein−protein interactions in cellular processes such as signal transduction and gene regulation has been well documented. One example is activation of basal transcription by activator protein-1 (AP-1), a heterodimeric Fos−Jun transcription factor that induces transcription of several genes, including human metallothionein IIa (MTIIa), collagenase, and interleukin 2 (IL2). Dimerization occurs by coiled-coil formation between a pair of helices on Fos and Jun, where the hydrophobic faces of these helices are buried to provide the energetic driving force for complex formation and charged residues surrounding the hydrophobic faces interact to provide the selectivity for heterodimer formation relative to either homodimer.[8,9] In contrast, the role of protein−protein interactions in the channeling of reactive intermediates from one active site to another in multifunctional enzyme systems has not been extensively explored and is only beginning to be appreciated.[13−16]

In earlier studies we have evaluated the role of protein−protein interactions in the selective channeling of intermediates between adjacent and nonadjacent modules of DEBS. At least three factors are known to influence the selectivity of chain transfer between modules. First, the KS domains of acceptor modules show selectivity for incoming substrates.[17−21] Second, acceptor KS domains also show selectivity for donor ACP domains.[6,22] Third, short segments at the adjacent C- and N-terminal ends of the three DEBS proteins (~100 residues at the C-termini of DEBS1 and DEBS2 and ~40 residues at the N-termini of DEBS2 and DEBS3) selectively interact to ensure accurate chain transfer between modules 2 and 3 and between modules 4 and 5.[4,5] Notably, these linker pairs (designated M2C and M3N, and M4C and M5N, respectively) represent modular units of recognition that are structurally and functionally independent from the catalytic domains of DEBS modules. Moreover, linker pair interactions can increase the maximum velocity (k_{cat}) of chain transfer of otherwise disfavored substrates by as much as 100-fold.[5] Therefore, in addition to providing new insights into the role of protein−protein interactions in multifunctional enzymes, a better understanding of the precise mechanisms of linker pair interactions could enhance the ability to rationally engineer novel polyketides by rewiring modules from naturally occurring PKS systems. Here we have used a combination of protein chemical, multidimensional NMR, and mutagenesis approaches to validate the "coiled-coil" model for linker pair interactions and to identify electrostatic interactions that contribute to the observed specificity of chain transfer between modules 2 and 3 of DEBS.

Nuclear magnetic resonance (NMR) spectroscopy is a powerful and informative tool to investigate higher order structures of peptides and polypeptides. In particular, nuclear Overhauser effect spectroscopy (NOESY) identifies atoms that are spatially close to one another. For small peptides, addition of trifluoroethanol (TFE) can stabilize otherwise transient secondary structural features. Given the anticipated short size of secondary structural elements in M3N, 10% TFE was added to the NMR sample of M3N. Figure 2B shows the predicted (i to $i + 3$ and i to $i + 4$) ion pairs that might be involved in intrahelical stabilization of M2C and M3N.[23−25] Addition of TFE presumably stabilizes these ionic interactions by lowering the dielectric

(13) Perham, R. N. *Biochemistry* **1991**, *30*, 8501−8512.
(14) Reed, L. J.; Hackert, M. L. *J. Biol. Chem.* **1990**, *265*, 8971−8974.
(15) Hengeveld, A. F.; Westphal, A. H.; de Kok, A. *Eur. J. Biochem.* **1997**, *250*, 260−268.
(16) Tsuji, S. Y.; Wu, N.; Khosla, C. *Biochemistry* **2001**, *40*, 2317−2325.
(17) Jacobsen, J. R.; Hutchinson, C. R.; Cane, D. E.; Khosla, C. *Science* **1997**, *277*, 367−369.
(18) Chuck, J.; McPherson, M.; Huang, H.; Jacobsen, J. R.; Khosla, C.; Cane, D. E. *Chem. Biol.* **1997**, *4*, 757−766.
(19) Wu, N.; Kudo, F.; Cane, D. E.; Khosla, C. *J. Am. Chem. Soc.* **2000**, *122*, 4847−4852.
(20) Holzbaur, I. E.; Ranganathan, A.; Thomas, I. P.; Kearney, D. J.; Reather, J. A.; Rudd, B. A.; Staunton, J.; Leadlay, P. F. *Chem. Biol.* **2001**, *8*, 329−340.
(21) Cane, D. E.; Kudo, F.; Kinoshita, K.; Khosla, C. *Chem. Biol.* **2002**, *9*, 131−142.
(22) Ranganathan, A.; Timoney, M.; Bycroft, M.; Cortes, J.; Thomas, I. P.; Wilkinson, B.; Kellenberger, L.; Hanefeld, U.; Galloway, I. S.; Staunton, J.; Leadlay, P. F. *Chem. Biol.* **1999**, *6*, 731−741.
(23) Marqusee, S.; Baldwin, R. L. *Proc. Natl. Acad. Sci. U.S.A.* **1987**, *84*, 8898−8902.
(24) Spek, E. J.; Bui, A. H.; Lu, M.; Kallenbach, N. R. *Protein Sci.* **1998**, *7*, 2431−2437.
(25) Hendsch, Z. S.; Tidor, B. *Protein Sci.* **1999**, *8*, 1381−1392.

constant of the solution,[26] thereby reducing line broadening. The observed ^{1}H NOE connectivities in the NOESY spectrum of M3N are summarized in Figure 3A and are strongly indicative of helical propensity in the linker, which is a prerequisite for coiled-coil formation. We note that the observed ^{1}H−^{1}H connectivity is incomplete; this could either be due to overlapping NOEs, which precluded unambiguous assignments, or to a loose structure resulting from the small size of the peptide or the absence of a partner peptide to stabilize the coiled-coil interaction.

Cysteine-mediated cross-linking is a well-established method for investigating intermolecular contacts between two proteins.[27] In particular, this technique has been used to determine the relative orientation of helices in a coiled coil.[8−10] Therefore, cysteine residues were engineered at selected positions in the linker regions of ACP2 and M3+TE proteins. The results shown in Figure 4B confirm that Y10 and T15 residues on the putative M3N helix come within 5 Å of the V3505 in the putative M2C helix. Thus, the helices must adopt an antiparallel orientation.

Although coiled coils are stabilized by general hydrophobic interactions, specificity is usually derived via ion-pair interactions. To identify charged residues that influence interactions between the putative M2C and M3N helices, we performed site-directed mutagenesis at selected residues. The R24E mutation in M3+TE substantially impaired the ability of M2 to transfer its triketide product to M3+TE. Concomitantly, a modest (2-fold) reduction in the intrinsic activity of M3+TE was observed, possibly due to the introduction of a negatively charged residue that destabilizes an intrahelical i , $i + 3$ ion pair in M3N (Figure 2B). A compensating E3496R mutation in M2C was able to partially restore chain transfer efficiency to the R24E mutant of M3+TE. Remarkably, chain transfer between the E3496R mutant of M2 and wild-type M3+TE was slightly improved compared to the wild-type protein pair. While not readily explicable, this finding reinforces the vital role of the linker pairs in intermodular chain transfer. Moreover, it suggests that although naturally occurring linker pairs are effective conduits for chain transfer, their properties could be further enhanced by protein engineering.

In conclusion, our results demonstrate, using a combination of protein chemical, structural, and mutagenesis approaches, that antiparallel helical interactions between intermodular linkers play an important role in chain transfer of a growing polyketide chain. Although further higher-resolution structural studies will be required to validate the coiled-coil model proposed here (Figure 2), our studies verify that intermodular interactions in PKSs can be altered in a modular fashion by manipulating linker pairs that mediate the interaction of noncovalently associated modules. While constructing chimeric modular PKS systems, two potential problems could be encountered: first, low expression of heterologous modules may result in an unfavorable shift in the association equilibrium between upstream and downstream modules. Second, naturally associating donor ACP and acceptor KS domains have recently been shown to have affinity for each other;[6] substitution of either the upstream or downstream module with a heterologous module could increase the K_D for module association. Designing high-affinity linker pairs could attenuate both these problems. Further structural and mechanistic studies on linker pairs from DEBS and other modular PKS systems are therefore warranted.

Materials and Methods

Reagents and Chemicals. DL-[2-*methyl*-^{14}C]Methylmalonyl-CoA (56.4 mCi/mmol) was obtained from ARC, Inc. The N-terminal linker of M3 (hereafter referred to as the M3N linker) was synthesized by New England Peptide (Fitchburg, MA), and had the following sequence: H_2N-MTDSEKVAEYLRRATLDLRAARQRIRELESD-amide.

Plasmid Construction and Mutagenesis. Plasmid pPK22, a pET28-(a) derivative, encodes DEBS module2 (M2) with both N- and C-terminal 6×-histidine tags, and is a derivative of pNW1,[28] where the DNA encoding the thioesterase domain was replaced with a *Spe*I−*Eco*RI fragment encoding the natural C-terminal linker of DEBS1. Plasmid pRSG34, encoding module 3 of DEBS fused to the thioesterase (TE) domain (M3+TE), has been described earlier.[3]

Mutagenesis of the genes encoding ACP2, M2, and M3+TE on pNW2, pPK22, and pRSG34, respectively, was performed with the QuikChangeXL kit (Stratagene). Oligonucleotides and plasmids used are listed as Supporting Information. The accuracy of mutant plasmids was confirmed by sequencing, followed by subcloning of the sequenced region into authentic vectors. A FLAG tag (encoded by the DYKD-DDDK sequence) was also introduced at the N-terminal end of ACP2 for purification and unambiguous identification of an ACP2−M3+TE adduct by Western blotting.

Strains and Culture Conditions. Expression of proteins for kinetic analysis was achieved by using the above plasmids to transform BAP1, an engineered strain of *Escherichia coli* BL21(DE3) containing a chromosomally integrated copy of the *sfp* phosphopantetheinyl transferase gene from *Bacillus subtilis*.[29] The *sfp* gene product was required for posttranslational phosphopantetheinylation of the ACP domains of individual modules. Proteins for cross-linking experiments, however, were expressed in BL21 cells so that background cross-linking at active sites of ACP could be avoided. Cells expressing M2 and its mutant (E3496R) were selected with kanamycin, whereas those expressing wild-type and mutant (V3483C and V3505C) ACP2 proteins as well as M3+TE and its mutants (R24E, Y10C, T15C) were selected with carbenicillin. Starter cultures of 10−20 mL of LB medium were inoculated and grown at 37 °C. After 6 h, the cells were pelleted and used to inoculate two 2 L flasks containing 1 L of LB medium each. The flasks were shaken at 250 rpm at 37 °C until the culture optical density at 600 nm (OD_{600}) was 0.6. At this point the flasks were placed in a water bath to cool the cells to 22 °C (ca. 10 min) and then induced with 0.1 mM isopropyl β-D-thiogalactopyranoside at an $OD_{600} = 0.8$. Flasks were then shaken at 22 °C for 15 h.

Purification of Proteins. Wild-type M3+TE and its mutant were purified as described by Tsuji et al.[4] For the purification of wild-type M2 and its mutant, cells were harvested by centrifugation and resuspended in Ni−NTA loading buffer (50 mM Tris, 300 mM NaCl, 1 mM EDTA, and 20% glycerol, pH 8.0). Cells were lysed at 1000 psi in a French press and centrifuged for 45 min at 33300*g*. The supernatant was batch-loaded onto 5 mL of Ni−NTA-Superflow resin (Qiagen) for 45 min. The Ni−NTA matrix-bound protein was packed into a Flex-column (Kontes), and the Ni−NTA resin was washed with 30 mL of loading buffer followed by 15 mL of wash buffer (loading buffer + 10 mM imidazole). The protein was eluted with 15 mL of elution buffer (loading buffer + 100 mM imidazole). DTT was added to a final

(26) Myers, J. K.; Pace; C. N.; Scholtz, J. M. *Protein Sci.* **1998**, *7*, 383−388.
(27) Pieper, R.; Gokhale, R. S.; Luo, G.; Cane, D. E.; Khosla, C. *Biochemistry* **1997**, *36*, 1846−1851.
(28) pNW1 is a derivative of M2 encoding pBP19, where the natural M2C linker has been replaced with a thioesterase domain and the resulting M2+TE was cloned into pET28. The resulting M2+TE contains both N- and C-terminal 6× histidine tags.
(29) Lambalot, R. H.; Gehring, A. M.; Flugel, R. S.; Zuber, P.; LaCelle, M.; Marahiel, M. A.; Reid, R.; Khosla, C.; Walsh, C. T. *Chem. Biol.* **1996**, *3*, 923−936.

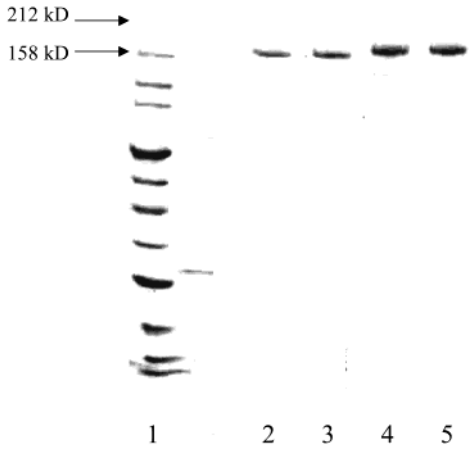

Figure 5. Purity and concentrations of proteins were determined by Lowry and densitometric analysis. Equimolar amounts of all proteins were loaded on the SDS−polyacrylamide gel. Lane 1, protein marker; lane 2, wild-type M2; lane 3, E3496R M2; lane 3, wild-type M3+TE; lane 4, R24E M3+TE. All proteins were >90% pure.

concentration of 2.5 mM immediately after elution of the protein. The eluted protein was about 50% pure and was concentrated to 1 mL by use of Centriprep 50 membranes (50 kDa molecular mass cutoff; Amicon). Following concentration, 19 mL of buffer A [100 mM sodium phosphate (pH 7.2), 2.5 mM DTT, 1 mM EDTA, and 20% (v/v) glycerol] was added to the protein and the resulting solution was applied to an anion-exchange column (Resource Q, 6 mL, Pharmacia) at 1 mL/min. A gradient of 0−0.15 M NaCl in buffer A was run at 1 mL/min for three column volumes, followed by a gentle gradient of 0.15−0.30 M NaCl at 1 mL/min for 10 column volumes. Fractions (3 mL) were collected, and those containing concentrated protein (typically 0.22−0.25 M NaCl) were pooled and further concentrated by use of Centriprep 50 membranes to a concentration of 2−4 mg/mL. Protein concentrations were measured via the modified Lowry assay (Sigma) as well as densitometric analysis of SDS−PAGE gels stained with Coomassie Blue. On the basis of the densitometry data, all proteins were determined to be >90% pure (Figure 5).

For the purification of FLAG-tagged ACP proteins, cells were harvested and resuspended in buffer A [100 mM sodium phosphate (pH 7.2) and 1 mM EDTA]. Cells were lysed at 1000 psi in a French press and centrifuged for 45 min at 33300*g*. DNA was precipitated by adding poly(ethylenimine) (PEI; to a final concentration of 0.15%) followed by centrifugation for 20 min at 33300*g*. Proteins were then applied to an anion-exchange column (HiTrap Q, 5 mL, Pharmacia) at 1 mL/min. A gradient of 0−0.50 M NaCl in buffer A was run at 1 mL/min for 10 column volumes. Fractions (3 mL) were collected, and those containing concentrated protein (typically 0.2−0.4 M NaCl) were pooled. The resulting solution was applied to a Flex-column packed with FLAG agarose (Sigma). After loading, the protein column was washed with wash buffer (buffer A + 300 mM NaCl) until no protein was detected by Bradford assay (Bio-Rad). ACP2 was then eluted with 20 mL of 100 μg/mL FLAG peptide (Sigma) in wash buffer. Eluted protein was >95% pure. It was concentrated and buffer-exchanged with storage buffer (100 mM sodium phosphate, 1 mM EDTA, and 20% glycerol).

NMR Spectroscopy. The M3N peptide was dissolved in 20 mM sodium phosphate and 10% D_2O, pH 5.5, to a final concentration of 3 mM. Trifluoroethanol (10%) was also added to promote helix formation.[26] The WET pulse sequence was used to suppress the water signal. Both NOESY and TOCSY spectra were acquired; the former was used to analyze secondary structure, whereas the latter enabled unambiguous assignment of relevant peaks. The spectra were recorded on a Varian 500 MHz spectrometer.

Chemical Cross-Linking. The contact surface and orientation of ACP2 and M3+TE was assayed in a cross-linking assay in which freshly purified 1,3-dibromopropanone was used as a bifunctional cross-linking reagent. In each assay, 1 μM M3+TE and 100 μM ACP2 were used. 1,3-Dibromopropanone was added to a final concentration of 10 mM in the enzyme mixture (50 μL volume). After 10 min the reaction was quenched with addition of DTT to a final concentration of 25 mM. The proteins were then denatured and loaded on two 4−15% gradient polyacrylamide gels. One of the gels was stained with Coomassie Blue, and the other one was subjected to Western blotting procedures to unambiguously identify the locations of the FLAG-tagged ACP2 protein. For Western blotting, the proteins were transferred to a nitrocellulose membrane. Blots were blocked in PBS containing 1% nonfat milk powder. ACP2 was detected with anti-FLAG antibody (Sigma, 1:1000 dilution), followed by peroxidase-conjugated secondary antibodies (1:1000 dilution). Proteins were visualized with the ECL kit (Amersham Pharmacia Biotech).

In Vitro Assays for Polyketide Production. The ability of M2 and M3+TE to productively associate was measured by an assay in which the *N*-acetylcysteamine thioester of (2*S*,3*R*)-2-methyl-3-hydroxypentanoic acid diketide (**2**, NDK), a mimic of the natural diketide substrate of M2 (Figure 1B), was converted into the expected tetraketide product **3** in the presence of methylmalonyl-CoA and NADPH. In addition to the two proteins themselves, assays for chain transfer and elongation between M2 and M3+TE contained 7 mM NDK, 0.5 mM [^{14}C]-methylmalonyl-CoA (only the 2*S* stereoisomer is active, and specific activity is reduced to 3.4 mCi/mmol), 4 mM NADPH, 440 mM sodium phosphate, 1 mM EDTA, 2.5 mM DTT, and 20% (w/v) glycerol, pH 7.2, in 70 μL.[4]

Computer Simulation of the Proposed "Coiled-Coil". To evaluate the potential mode(s) of interaction between M2C and M3N, a computer model based on the "coiled-coil" mode of interaction proposed earlier[4] was developed with the Swiss PDB Viewer software. Both parallel and antiparallel orientations were explored. Φ and Ψ angles for each residue were chosen such that their values lie in the α-helical region on the Ramachandran plot. Energy minimization of individual coils was performed to make sure that the helical conformation is energetically feasible. Rotamers for the important charged residues were selected such that they come close to each other without any steric clashes with surrounding residues.

Acknowledgment. This research was supported by grants from the NIH to C.K. (CA66736) and D.E.C. (GM 22172). We also thank Stephen Lynch and Corey Liu for their help in setting up NMR experiments and Sheryl Tsai for her help in computer modeling of the coiled-coil.

Supporting Information Available: TOCSY and NOESY NMR spectra of peptide M3N and associated assignments, and sequences of oligonucleotides and plasmids used for linker mutagenesis. This material is available free of charge via the Internet at http://pubs.acs.org.

JA0297537